Inclusive (p, Δ^{++}) and $(p, p'\pi^+)$ reactions

B. K. Jain and Neelima G. Kelkar
Nuclear Physics Division, Bhabha Atomic Research Center, Bombay, 400 085, India

J. T. Londergan
Nuclear Theory Center, Indiana University, Bloomington, Indiana 47405
(Received 28 August 1992)

Formulas are derived for cross sections for inclusive (p, Δ^{++}) and $(p, p'\pi^+)$ reactions; these are shown to depend on the pion self-energy in the nucleus, and the production and decay vertices of the Δ^{++}. The pion self-energy includes both nucleon excitation (NN^{-1}) as well as delta excitation (ΔN^{-1}) in the nucleus. The pion-nucleon couplings in the transition vertex as well as in the self-energy are written using relativistic pseudovector coupling; results are compared with a nonrelativistic reduction. The distortions of the continuum particles are included in a "distorted-wave Fermi gas" approximation. Calculations are made for the excitation spectrum of the nucleus, $d\sigma/d\omega$, and the angular distribution in the (p, Δ^{++}) reaction, for proton beam energies from threshold to 3 GeV. For the $(p, p'\pi^+)$ reaction cross sections are calculated for the proton spectrum and the distribution $d\sigma/d\Omega_\pi \Omega p' dE_{p'} dE_\pi$ at fixed values of the proton and pion angles and a fixed value of $E_{p'}$. The latter essentially gives the excitation energy spectrum of the nucleus. Many interesting features are seen in these spectra. The differences in results using relativistic pion-nucleon coupling and its nonrelativistic reduction are shown to increase with the beam energy. Around 400 MeV, there is little difference in the cross sections but at 1 GeV and beyond the difference becomes large, changing both the magnitude and shape of the distributions. The inclusion of distortions reduces the magnitude of the cross section but leaves the shape unchanged.

PACS number(s): 25.40.Ve, 14.20.Gk, 21.65.+f, 24.10.Jv

I. INTRODUCTION

A wide variety of nuclear reactions at intermediate energies can be well described using nucleons, pions, and deltas as the "elementary" degrees of freedom [1]. Using this approach one can obtain a quantitative description of various nuclear reactions induced by pions and nucleons, though the precise form of the delta-nucleus interaction remains a major uncertainty in these descriptions [2, 3]. In the past few years there has been great interest in performing experiments where the $\Delta(1232)$ isobar is produced explicitly; the aim is to directly measure the nuclear effects in isobar production. Since the Δ is a spin-isospin excitation of the nucleon, much of this experimental work has been done with charge-exchange reactions which show strong selectivity for Δ excitation. Measured inclusive energy spectra of neutrons in (p, n) reactions [4], and tritons in $(^3\mathrm{He}, t)$ reactions [5, 6], on targets ranging from ^{12}C to ^{208}Pb have shown broad bumps around 300 MeV excitation energy with large cross sections. They correspond to excitation of a nucleon in the target nucleus to a delta isobar. Similar Δ excitations have also been seen in heavy-ion charge-exchange reactions [7] like $(^{12}\mathrm{C}, {}^{12}\mathrm{N})$, $(^{16}\mathrm{O}, {}^{16}\mathrm{N})$, and $(^{20}\mathrm{Ne}, {}^{20}\mathrm{F})$.

In the above experiments, Δ is produced in the nuclear environment, so the relevant measurements are not made on an isolated delta, or its decay products (nucleon and pion). Thus these data are suited to explore the real delta-nucleon hole (ΔN^{-1}) excitations in nuclei and thereby the collective aspects of these modes. To date probably the most dramatic result in these reactions is the observed shift in the position of the Δ peak, relative to the position of the same peak on a hydrogen target. It is generally interpreted as a manifestation of the effect of Δ-nucleus collective dynamics, though this interpretation is not firm [8]. To resolve this question a second generation of experiments have been done recently at KEK and Saturne [9], where the triton in $(^3\mathrm{He}, t)$ and neutron in (p, n) reactions are seen in coincidence with various charged particles like π^+, pp, $\pi^+ p$, etc. The data where the $\pi^+ p$ are measured in coincidence do not appear to show any shift from the free Δ peak.

Another class of intermediate energy reactions are those where the Δ appears as one of the final reaction products, and its properties can therefore be measured directly. In a few cases the presence of the Δ can be inferred by measuring the recoiling nucleus, as in the pioneering experiment on the ^{6}Li, $(p, \Delta^{++})^6$He reaction at Saturne [10]. A second type of reaction measures the ejectile nucleus on proton targets, as in the experiments on $p(^3\mathrm{He}, t)\Delta^{++}$ or $p(^{12}\mathrm{C}, {}^{12}\mathrm{B})\Delta^{++}$ reactions, carried out at Saturne and Dubna [5–7, 11]. These measurements are suitable for studying the delta-nucleus interaction in the continuum and the transition interaction $pp \rightarrow n\Delta^{++}$.

Furthermore, as the Δ is a spin-isospin 3/2 excitation of the nucleon with large momentum mismatch and with an excitation energy of roughly 300 MeV, Δ production reactions provide a way to study spin-isospin modes in nuclei which correspond to single or double spin-isospin flip at large momentum transfer. In situa-

tions where the final nuclear spectrum has only a single particle-stable state one explores the exclusive transition density corresponding to this state; otherwise the data determine the transition density inclusive of all particle bound states. Inspired by such a strong physics potential of the (p, Δ^{++}) reaction extensive theoretical efforts have been made to understand its reaction mechanism and identify a consistent theoretical framework for analyzing the data [12–14]. It has been found that this reaction proceeds in one step and the measured cross sections can be adequately described in the framework of the distorted-wave Born approximation (DWBA). It has also been found that, due to very large momentum transfer ($\sim$ beam momentum) involved in the excitation of a bound proton in the initial state to Δ^{++} in the continuum in the final state, the "target excitation" amplitude in the (p, Δ^{++}) reaction contributes little beyond 1 GeV beam energy [15].

Another way to study experimentally the (p, Δ^{++}) reaction is to detect directly the Δ^{++} through coincidence measurement of its decay products p and π^+. This procedure has the great advantage that the reaction can be performed on any target nucleus. The experiments would lead to inclusive measurements because here the residual nucleus can be in any state, including particle-unstable states. The data would explore the full spin-isospin response of the nucleus in the momentum transfer domain beyond about 300 MeV/c.

The energy transfer to the nucleus in these inclusive measurements can vary from small to very large by choosing different energies of the outgoing delta. This response could be very different from that in the (p, n) or (p, p') reactions, where the relation between energy and momentum transferred to the nucleus follows the free one-nucleon dispersion relation. The nature of the response could also be different because as an unstable resonant state, the Δ has a mass distribution. For a given energy transfer, this leads to an integral over a range of momentum transfer to the nucleus.

In the present paper we have studied the inclusive (p, Δ^{++}) and $(p, p'\pi^+)$ reactions in nuclei. Guided by previous theoretical work [12–14] we assume that Δ^{++} excitation proceeds in one step and only the excitation of the projectile proton contributes (i.e., we neglect the "target excitation" contribution arising from excitation of a target nucleon to a Δ). The $p \rightarrow \Delta^{++}$ transition is described by the one-pion relativistic pseudovector Lagrangian with appropriate form factor at the vertex. The distortion of the continuum proton and the delta are described in the eikonal approximation which, as has been shown recently by Kelkar and Jain [16], compares well with the exact solution of the Schrödinger wave equation in the present case. The response of the nucleus is described by a "distorted-wave Fermi gas model" [17]. The pion propagator in the nuclear medium is written relativistically. Calculations are made for various differential cross sections with a proton beam which goes from low energy, around 400 MeV, to 3 GeV. For comparison we have also used nonrelativistic expressions for the coupling of the pion.

We have used the longitudinal contribution from π exchange to describe the spin-averaged $p \rightarrow \Delta^{++}$ transition. We have not included the tranverse contribution from ρ exchange. The detailed experimental studies by Wicklund *et al.* [18] clearly demonstrate that pion exchange gives a very good fit to the free (p, Δ^{++}) reaction over a wide kinematic region. The spin-averaged (p, Δ) data are reproduced rather well by a model which includes π exchange but subtracts off the contributions from small impact parameter [12, 19]. In our calculation we use a Landau-Migdal term to incorporate short-ranged repulsion in the hadronic interaction; this should give a very good approximation to the spin-averaged (p, Δ) reaction.

A second reason for omitting ρ exchange is that attempts to include this in the $pp \rightarrow n\Delta^{++}$ reaction have obtained very unsatisfactory results. A recent detailed study by Jain and Santra [20] and earlier work by Dmitriev, Suskov, and Gaarde [12] both showed that the experimental data on this reaction are better described by one-pion exchange only. Thus either the strength of the $\rho N\Delta$ coupling, $f_{\rho N\Delta}$, is considerably weaker than is usually assumed, or some additional amplitude tends to cancel the contribution from the ρ. Finally, $(\vec{d}, 2p)$ experiments by Ellegaard *et al.* [19] suggested a very large transverse component in the $NN \rightarrow N\Delta$ reaction; however Sams and Dmitriev have shown [21] that the large transverse contribution arises from deuteron distortion effects, and thus would not be present in our reaction. In view of these facts we have not considered ρ exchange in the spin-averaged $p \rightarrow \Delta^{++}$ transition.

In our model, the $(p, p'\pi^+)$ reaction is produced by the decay of the Δ^{++}. Since the isobar is produced with large kinetic energy, we assume that nuclear distortions do not significantly affect the mass distribution of the Δ or its subsequent decay into p and π^+.

Before concluding this section we note that the final state in the $(p, p'\pi^+)$ reaction contains at least three free particles. In principle we must consider the interaction between the final p' and π^+ with each other, and also their interactions with the recoiling nucleus. However, if we restrict ourselves to experimental situations where the available energy of the $p'\pi^+$ system is in the range of the delta mass, the dominant effect of the interaction between p' and π^+ is the production of the Δ^{++}. In that case the remaining final state interactions can also be described reasonably well by considering the interaction of the Δ^{++} with the recoiling nucleus. Thus our model calculations on the $(p, p'\pi^+)$ reaction, presented in this paper, should be applicable in the kinematic region when the invariant mass of the $p'\pi^+$ system is close to the central mass of the Δ^{++} (1232 MeV). Because of this the preemission pion diagram also would contribute little to the $(p, p'\pi^+)$ reaction in the region of the applicability of our model.

In Sec. II we give the formalism for inclusive (p, Δ^{++}) reactions. Initially we derive expressions for the transition amplitude using plane waves for the proton and delta and further include the effects of distortion. We discuss the results and study the behavior of various cross sections and thereby the response of the nucleus at incident proton energies from threshold to 3 GeV. We also study

the missing mass spectra for the inclusive (p,Δ^{++}) reaction which show trends similar to that in the exclusive (p,Δ^{++}) reaction.

In Sec. III we study the inclusive $(p,p'\pi^+)$ reaction. The formalism is similar to that for the (p,Δ^{++}) reaction, and the cross section is written in terms of the one-pion-exchange interaction, delta propagator, its decay vertex, and the nuclear response. In both cases we compare results using the relativistic and nonrelativistic pion-nucleon couplings. We calculate the inclusive proton energy spectrum for the $(p,p'\pi^+)$ reaction. As our work is exploratory in nature, we also study the other possible differential cross sections in different kinematic regions, which may prove useful in planning future experiments.

II. INCLUSIVE (p,Δ^{++}) REACTIONS

A. Formalism

In an inclusive (p,Δ^{++}) reaction on the nucleus, the nucleus is left in any state consistent with the kinematics. The cross section for the inclusive (p,Δ^{++}) reaction on a spin-zero nucleus is written in terms of the transition amplitude, T_{n0}, where n is the excited state of the nucleus and 0 the ground state of the target nucleus, as

$$d\sigma = \frac{2\pi}{\hbar v_p}\frac{m_p m_\Delta}{E_p E_\Delta}\frac{d\mathbf{k}_\Delta}{(2\pi)^3}\sum_n \delta(\omega-\omega_n)\frac{1}{2}\sum_{\sigma_p\sigma_\Delta}|T_{n0}|^2. \tag{1}$$

Here E_p and E_Δ are the energies of the incident proton and outgoing delta and $\omega = E_p - E_\Delta$ is the energy transferred to the nucleus. In DWBA the transition matrix T_{n0} has the form

$$T_{n0}(\mathbf{k}_\Delta,\mathbf{k}_p) = \left(\chi^-_{k_\Delta}, \left\langle n,\Delta^{++}\left|\sum_i V_{\sigma\tau}(i)\mathbf{T}^+\cdot\boldsymbol{\tau}(i)\right|p,0\right\rangle, \chi^+_{kp}\right). \tag{2}$$

Here χ's denote distorted waves for the proton and delta. $V_{\sigma\tau}$ is the spin-isospin interaction which, in the nonrelativistic version of the one-pion-exchange potential, is written as

$$V_{\sigma\tau}(i) = V(\omega,\mathbf{q})\mathbf{S}^+\cdot\hat{\mathbf{q}}H_{\pi NN}(i), \tag{3}$$

where $V(\omega,\mathbf{q})\mathbf{S}^+\cdot\hat{\mathbf{q}}$ is the transition vertex along with the pion propagator for the $p\rightarrow\Delta^{++}$ transition, i.e.,

$$V(\omega,\mathbf{q}) = -\frac{f^*}{m_\pi}F^*(t)\frac{|\mathbf{q}|}{m_\pi^2-t}, \tag{4}$$

$\mathbf{T}$ and $\mathbf{S}$ are the isospin and spin transition operators, respectively, for the transition $1/2\rightarrow 3/2$. In Eq. (3) $H_{\pi NN}$ is the nuclear pion-nucleon coupling vertex,

$$H_{\pi NN} = \frac{f}{m_\pi}F(t)\boldsymbol{\sigma}\cdot\mathbf{q}. \tag{5}$$

If the nucleon in the nucleus is excited to a Δ, the pion-nucleon vertex $H_{\pi NN}$ is replaced by $H_{\pi N\Delta}$. The relativistic version of the above interaction will be considered later. ω and $\mathbf{q}$ are the energy and momentum transfer and $t=(\omega^2-|\mathbf{q}|^2)$ is the four-momentum transfer. f (f^*) and $F(t)$ ($F^*(t)$) denote the bare coupling and form factor, respectively, for the πNN ($\pi N\Delta$) vertex. The values of the coupling constants are taken as $f=1.0026$ and $f^*=2.1562$. The form factors F and F^* are described by a monopole form:

$$F(t) = \frac{\Lambda^2-m_\pi^2}{\Lambda^2-t}, \tag{6}$$

where the cutoff parameter, Λ, gives a measure of its extension. On the choice of the values of this parameter there is no definite agreement. However a value of 1 GeV/c or larger seems essential for explaining some fundamental nuclear physics phenomena like deuteron properties [22] ($1.0<\Lambda<1.4$ GeV/c), $N-N$ scattering data [23] ($0.9<\Lambda<1.4$ GeV/c), and $pp\rightarrow n\Delta^{++}$ transition data [24] ($\Lambda\sim 1.0$–1.2 GeV/c). We therefore use $\Lambda=1.2$ GeV/c. However, we also present some calculated cross sections for comparison using $\Lambda=0.65$ GeV/c, a value nearer to that obtained with quark models [25] and the plane-wave Born approximation (PWBA) analysis of the $pp\rightarrow n\Delta^{++}$ transition data [12].

To evaluate Eq. (2), we first write the distorted waves in momentum space, giving

$$T_{n0}(\mathbf{k}_\Delta,\mathbf{k}_p) = \int d\mathbf{k}'_p d\mathbf{k}'_\Delta \chi^{-*}_{k_\Delta}(\mathbf{k}'_\Delta)\chi^+_{k_p}(\mathbf{k}'_p)\times\left(\mathbf{k}'_\Delta,\left\langle n,\Delta^{++}\left|\sum_i V_{\sigma\tau}(i)\mathbf{T}^+\cdot\boldsymbol{\tau}(i)\right|p,0\right\rangle,\mathbf{k}'_p\right), \tag{7}$$

where $\mathbf{k}'_i$ denotes the momentum of the subscripted particle in the medium. Analogous to $\mathbf{q}$, the momentum transfer $\mathbf{q}'$ corresponding to the local momenta is

$$\mathbf{q}' = \mathbf{k}'_p - \mathbf{k}'_\Delta. \tag{8}$$

To simplify evaluation of Eq. (7) we now observe the following.

(i) The energy region of the beam is around 1 GeV and beyond. At these energies the local momenta $\mathbf{k}'_p$ and $\mathbf{k}'_\Delta$ of the continuum particles do not differ much from their asymptotic values.

(ii) The momentum transfer, $\mathbf{q}$, in the (p,Δ^{++}) reaction is large (>250 MeV/c).

(iii) As shown previously by Jain [14], the momentum dependence of the transition interaction $V_{\sigma\tau}$ in this high momentum range is weak.

In view of these reasons one can reasonably approximate the interaction $V(\omega,q)$ in Eq. (2) by its values corresponding to the asymptotic momentum transfer $\mathbf{q}$ ($=\mathbf{k}_p-\mathbf{k}_\Delta$). This approximation factorizes T_{n0} as

$$T_{n0}(\mathbf{k}_\Delta,\mathbf{k}_p) \equiv V(\omega,\mathbf{q})\langle\Delta^{++}|\mathbf{S}^\dagger\cdot\hat{\mathbf{q}}\mathbf{T}^\dagger_+|p\rangle F_{n0}(-q), \tag{9}$$

where

$$F_{n0}(-q) = \left\langle n \left| \sum_i \chi^{-*}_{k_\Delta}(\mathbf{r}_i)\chi^{+}_{k_p}(\mathbf{r}_i) H_{\pi NN}(i)\tau_-(i) \right| 0 \right\rangle = \int d\mathbf{r}\chi^{-*}_{k_\Delta}(\mathbf{r})\chi^{+}_{k_p}(\mathbf{r})\rho_{n0}(\mathbf{r}) \quad (10)$$

with

$$\rho_{n0}(\mathbf{r}) = \left\langle n \left| \sum_i \delta(\mathbf{r}-\mathbf{r}_i) H_{\pi NN}(i)\tau_-(i) \right| 0 \right\rangle. \quad (11)$$

Now substituting Eq. (9) for T_{n0} we obtain

$$\sum_n \delta(\omega-\omega_n) \sum_{\sigma_p\sigma_\Delta} |T_{n0}|^2 = \frac{4}{3}|V(\omega,\mathbf{q})|^2 \left[\sum_n \delta(\omega-\omega_n)|F_{n0}(-q)|^2 \right], \quad (12)$$

where the term in the square brackets is the dynamical structure factor and is commonly denoted by $S(\mathbf{q},\omega)$.

$$S(\mathbf{q},\omega) \equiv \sum_n \delta(\omega-\omega_n)|F_{n0}(-q)|^2 = \sum_n \delta(\omega-\omega_n) \left| \left\langle n \left| \sum_i e^{i\mathbf{q}\cdot\mathbf{r}_i} H_{\pi NN}(i)\tau_-(i) \right| 0 \right\rangle \right|^2. \quad (13)$$

In an approximation of nuclear matter to the nucleus $S(\mathbf{q},\omega)$ can be further written as

$$S(\mathbf{q},\omega) = -\frac{\mathcal{V}}{\pi}\mathrm{Im}\ \Pi(\mathbf{q},\omega), \quad (14)$$

where $\mathcal{V}$ is the nuclear volume. The factor $\mathcal{V}$ indicates that in the nuclear matter description we can only talk of a quantity per unit volume. For a nucleus of a given number of protons, Z, and density ρ_0, we can write

$$\mathcal{V} = Z/\rho_0 = \frac{3\pi^2}{k_F^3}Z. \quad (15)$$

$\Pi(\omega,\mathbf{q})$, is the pion self-energy in the nuclear medium and is related to its susceptibility $\chi_\pi(\omega,\mathbf{q})$ through

$$\Pi(\mathbf{q},\omega) = -|\mathbf{q}|^2\chi(\mathbf{q},\omega). \quad (16)$$

In the relativistic form we replace $(-q^2)$ by t.

In arriving at the final form Eq. (14), we have followed Fetter and Walecka [26] and also used the identity

$$\lim_{\eta\to 0}\int_a^b \frac{F(n)dn}{n-n_0\mp i\eta} = P\int_a^b \frac{F(n)}{n-n_0}dn \pm i\pi\delta(n-n_0)F(n_0). \quad (17)$$

For the Fermi gas approximation to the nuclear medium, expressions for $\Pi(\omega,\mathbf{q})$ have been derived in the literature [3, 27].

In the present paper we are considering beam energies up to 3 GeV; at these energies a large amount of the beam energy remains, even after giving away 300 MeV to excite the projectile proton to a Δ. This energy could be transferred to the nucleus. Therefore, while considering the self-energy of the pion in the nucleus, we should also include nuclear delta-hole (ΔN^{-1}) excitations, writing thereby in Eq. (14)

$$\Pi(\mathbf{q},\omega) = \Pi_N(\mathbf{q},\omega) + \Pi_\Delta(\mathbf{q},\omega), \quad (18)$$

where the subscripts denote the NN^{-1} and ΔN^{-1} contributions to the self-energy.

In the uncorrelated Fermi gas model for $\Pi(\omega,\mathbf{q})$, it is known that unphysical effects arise unless a short distance repulsion is included in the NN^{-1} or ΔN^{-1} state [3]. Normally this is done through introduction of the Migdal parameter, g', which supposedly mocks up these effects in the calculation of Π. In the special case where $g'_N = g'_\Delta = g'$, introduction of the Migdal parameter modifies the susceptibility to

$$\chi_N(\mathbf{q},\omega) \to \chi_N(\mathbf{q},\omega)/[1+g'(\chi_N+\chi_\Delta)], \quad \chi_\Delta(\mathbf{q},\omega) \to \chi_\Delta(\mathbf{q},\omega)/[1+g'(\chi_N+\chi_\Delta)]. \quad (19)$$

2. Distorted-wave description

In order to evaluate the expression $\sum_n \delta(\omega-\omega_n)|F_{n0}|^2$ including distortions we write the distorted waves in the eikonal approximation, i.e.,

$$\chi_k(\mathbf{r}) = e^{i\mathbf{k}\cdot\mathbf{r}}D_k(\mathbf{r}), \quad (20)$$

where D_k is the modulating function. It is given by

$$D_k^{(+)}(\mathbf{r}) = \exp\left[-\frac{i}{\hbar v}\int_{-\infty}^{z} V(\mathbf{b},z')dz'\right] \quad (21)$$

which defines it as the integral of the optical potential along the trajectory at impact parameter $\mathbf{b}$ and up to the point z. At the high beam energies considered here, scattering of the interacting particles in the continuum is predominantly in the forward direction, so the above approximation should be reasonably good. A recent calculation of the exclusive (p,Δ^{++}) reaction [16] has shown quantitatively that this is an accurate approximation. v in Eq. (21) is the asymptotic speed of the particle.

In the eikonal approximation, the product of distorted waves for the proton and Δ in Eq. (10) is written as

$$\chi^{-*}_{k_\Delta}(\mathbf{r})\chi^{+}_{k_p}(\mathbf{r}) \approx e^{iq_\parallel z}e^{i\mathbf{q}_\perp\cdot\mathbf{b}}e^{i\delta(\mathbf{b})}f(\mathbf{b},z), \quad (22)$$

where the momentum transfer $\mathbf{q} = (\mathbf{q}_\perp, q_\parallel)$. The subscripts $\perp$ and $\parallel$ denote the two-dimensional components perpendicular to the z axis and along the z direction, respectively. The eikonal phase $\delta(\mathbf{b})$ is defined as

$$\delta(\mathbf{b}) = -\frac{1}{\hbar v_p}\int_{-\infty}^{0} V_p(\mathbf{b},z)dz - \frac{1}{\hbar v_\Delta}\int_0^{\infty} V_\Delta(\mathbf{b},z)dz \tag{23}$$

and the factor $f(\mathbf{b},z)$ is given by

$$f(\mathbf{b},z) = \exp\left[i\int_0^z \left\{\frac{V_\Delta(\mathbf{b},z')}{\hbar v_\Delta} - \frac{V_p(\mathbf{b},z')}{\hbar v_p}\right\}dz'\right]. \tag{24}$$

In situations when V/v for the proton and Δ are equal, the term in curly brackets vanishes and $f(\mathbf{b},z)$ is unity. Recent calculations [20] have shown that the assumption $f(\mathbf{b},z) = 1$ is in fact quite accurate at the energies of interest in this paper; for the remainder of this paper, we therefore assume $f(\mathbf{b},z) = 1$. With this assumption, the product of the distorted waves in Eq. (22) depends only on $\mathbf{b}$; consequently the distortions affect the momentum transfer only in a plane perpendicular to z. The momentum transfer $q_\parallel$ occurs only at the hard collision $p \to \Delta^{++}$ transition vertex.

Using Eqs. (22)–(24) means that the effect of distortions on Eq. (14) gives

$$\frac{\pi}{\mathcal{V}}S(\mathbf{q},\omega) = -\int d\mathbf{b}\,d\mathbf{b}' e^{i\mathbf{q}_\perp\cdot(\mathbf{b}-\mathbf{b}')}e^{i[\delta(\mathbf{b})-\delta(\mathbf{b}')]}\mathrm{Im}\;\Pi(\mathbf{b}',\mathbf{b},q_\parallel,\omega), \tag{25}$$

where we have absorbed a factor $\exp[iq_\parallel(z-z')]$ to write the Fourier transform of Π in momentum space along the z direction.

To proceed further we follow Ref. [17] and evaluate Eq. (25) in a "distorted-wave Fermi gas model," and write

$$\Pi(\mathbf{b}',\mathbf{b},q_\parallel,\omega) = T^{1/2}(\mathbf{b})T^{1/2}(\mathbf{b}')\int\frac{d\mathbf{q}'_\perp}{(2\pi)^2}e^{i\mathbf{q}'_\perp\cdot(\mathbf{b}-\mathbf{b}')}\Pi(\mathbf{q}',\omega), \tag{26}$$

where $T(\mathbf{b})$ is the nuclear thickness function. In terms of the nuclear density ρ, it is given by

$$T(\mathbf{b}) = \int_{-\infty}^{+\infty}\rho(\mathbf{b},z)dz. \tag{27}$$

The Fermi gas pion self-energy Π in Eq. (26) is now evaluated at the momentum $q' = (q_\parallel^2+\mathbf{q}_\perp'^2)^{1/2}$. The range of $\mathbf{q}'_\perp$, as we shall see, is determined by the distortion factors. The normalization factors $T^{1/2}$ in Eq. (26) are necessary to relate the infinite Fermi gas geometry to our finite system.

Substituting Eq. (26) into Eq. (25) gives

$$\frac{\pi}{\mathcal{V}}S(\mathbf{q},\omega) = -\frac{1}{N_{\mathrm{eff}}}\mathrm{Im}\left[\int\frac{d\mathbf{q}'_\perp}{(2\pi)^2}\Pi(\mathbf{q}-\mathbf{q}'_\perp,\omega)|D(\mathbf{q}'_\perp)|^2\right], \tag{28}$$

where

$$D(\mathbf{q}'_\perp) = \int d\mathbf{b}\,e^{i\mathbf{q}'_\perp\cdot\mathbf{b}}e^{i\delta(\mathbf{b})}T^{1/2}(\mathbf{b}) \tag{29}$$

and

$$N_{\mathrm{eff}} = \int\frac{d\mathbf{q}'_\perp}{(2\pi)^2}|D(\mathbf{q}'_\perp)|^2. \tag{30}$$

The factor N_{eff} in Eq. (28) is introduced to ensure proper normalization.

3. *Relativistic pion-nucleon coupling*

The above expressions were derived using the nonrelativistic version of the pseudovector pion-nucleon Lagrangian coupling,

$$\mathcal{L}_{\mathrm{NR}} = \frac{f}{m_\pi}\chi_N\boldsymbol{\sigma}\cdot\mathbf{q}\boldsymbol{\tau}\chi_N\cdot\boldsymbol{\phi}_\pi + \frac{f^*}{m_\pi}\chi_\Delta\mathbf{S}^\dagger\cdot\mathbf{q}\mathbf{T}^\dagger\chi_N\cdot\boldsymbol{\phi}_\pi. \tag{31}$$

They can be easily modified for the relativistic Lagrangian

$$\mathcal{L}_{\mathrm{rel}} = \frac{f}{m_\pi}\bar\psi_N\gamma^\nu\gamma^5\boldsymbol{\tau}\psi_N\cdot\partial_\nu\boldsymbol{\phi}_\pi + \frac{f^*}{m_\pi}\bar\psi^\nu_\Delta\mathbf{T}\psi_N\cdot\partial_\nu\boldsymbol{\phi}_\pi, \tag{32}$$

where ψ_N represents the nucleon Dirac four-momentum spinors and ψ^ν_Δ represents the Δ spinor with covariant index ν, and χ_N and χ_Δ are the analogous two-component nonrelativistic wave functions. We obtain an expression corresponding to Eq. (12) for $\sum_n\delta(\omega-\omega_n)\sum|T_{n0}|^2$ by evaluating the $p\to\Delta^{++}$ transition with Eq. (32) and the self-energy, Π, for pions with $\mathcal{L}_{\mathrm{rel}}$. After some algebra one obtains

$$\sum_n\delta(\omega-\omega_n)\sum_{\sigma_p\sigma_\Delta}|T_{n0}|^2 = \frac{1}{3m_pm_\Delta}\left[t-\frac{(t-m_p^2+m_\Delta^2)^2}{4m_\Delta^2}\right]\left[t-(m_p+m_\Delta)^2\right]\left[\frac{f^*F^*(t)}{m_\pi}\frac{1}{m_\pi^2-t}\right]^2 S(\mathbf{q},\omega). \tag{33}$$

The structure factor $S(\mathbf{q},\omega)$ is written in the same form as in Eqs. (14) and (28), using the relativistic version of the self-energy derived using relativistic propagators, and the relativistic form of the $NN\pi$ and $\Delta N\pi$ vertices. The expressions for these have been derived in [3, 27].

B. Cross sections

The inclusive cross section for the (p,Δ^{++}) reaction in the center of mass is given by

$$\frac{d^3\sigma}{d(\mu^2)d\Omega\, d\omega} = \frac{E_A m_p \mu}{(2\pi)^2 E_c}\rho(\mu^2)\frac{k_\Delta}{k_p}\sum_n \delta(\omega-\omega_n)\frac{1}{2}\sum_{\sigma_p\sigma_\Delta}|T_{n0}|^2, \quad (34)$$

where μ is the variable mass of the Δ and $\rho(\mu^2)$ is its mass distribution function. We have used the same parametrization for $\rho(\mu^2)$ as given in a previous publication of ours [15]. ω is the energy transferred to the nucleus and Ω is the solid angle for the outgoing Δ. The transition amplitude has the form as described in Sec. II A; it contains the self-energy of the virtual pion, the interaction at the Δ production vertex, and the pion propagator. The parameters for the self-energy in the Fermi gas model are chosen as follows: we assume modification of the mass of the nucleon in the nuclear medium by taking a nucleon effective mass $m^* = 0.7m_N$. The value taken for the Fermi momentum is $k_F = 210$ MeV/c. The self-energies are written in terms of susceptibilities with Migdal parameters introduced to estimate the effects of short-ranged repulsion. We approximate $g'_N = g'_\Delta$ with the most commonly used value of 0.7. The double differential cross section, $d^2\sigma/d\Omega\, d\omega$, is constructed by integrating Eq. (34) over the allowed range of μ at each incident beam energy.

The missing mass spectrum $d\sigma/d(\mu^2)$ is calculated by integrating Eq. (34) over the allowed range of energy transferred and the allowed angles of the outgoing Δ. Using the kinematics appropriate to a nucleus of mass 16 we calculate the above cross sections at proton beam energies from 400 MeV to 3 GeV.

The distorting potential for the proton, which appears in the modulating function $D_{\mathbf{k}_p}$ of the eikonal approximation is calculated using the high energy ansatz. As the main effect of distortion is absorptive in the high energy region of interest [16] we consider only the imaginary part of the optical potential. The high energy expression for the potential V is given as follows:

$$V(r) = (i+\alpha)W_p\rho(r)/\rho(0), \quad (35)$$

where the imaginary part

$$W_p = -\frac{\hbar k_{pN}}{2\mu_{pN}}\sigma_T^{pN}\rho_0. \quad (36)$$

σ_T^{pN} is the proton-nucleon total scattering cross section, α is the ratio of real to imaginary parts of the proton-nucleon scattering amplitude, ρ_0 is the nuclear density, and k_{pN} and μ_{pN} are the momentum and reduced mass in the p-N center of mass. The function $\rho(r)/\rho(0)$ describes the radial dependence of the potential in terms of the nuclear density profile. To evaluate W_p, σ_T is taken from experimental data of proton scattering on nucleons [28, 29] and ρ_0 is taken as 0.17 fm^{-3}. With the above input the proton optical potentials at different energies are listed in Table I.

Unlike protons, not much information exists on the nuclear potential for the isobar. The kinetic energy T_Δ of the isobar, with a particular fixed mass, depends on the beam energy as well as the energy transfer (ω) to the nucleus. Therefore in an inclusive reaction, the Δ can be produced with any kinetic energy from zero to a few GeV. We thus require the Δ optical potential over a wide energy range.

For $T_\Delta < 60$ MeV we refer to the Δ-hole model of Hirata *et al.* [30] for a π-nucleus interaction in the region of the (3,3) resonance and take $W_\Delta = -45$ MeV. For $T_\Delta > 60$ MeV we make use of the high energy approximation of Eq. (36). The total cross section for the isobar is the sum of elastic and reaction parts, $\sigma_T^{\Delta N} = \sigma_{\rm el}^{\Delta N} + \sigma_r^{\Delta N}$. Assuming that the delta and proton elastic dynamics are not very different, we write $\sigma_{\rm el}^{\Delta N} \approx \sigma_{\rm el}^{NN}$. Since up to about $T_\Delta = 1.5$ GeV it is known that the main reactive channel in ΔN scattering is $\Delta N \to NN$ [29], then using the reciprocity theorem we write

$$\sigma_r^{\Delta N} \approx \sigma^{\Delta N\to NN} = \frac{1}{2}\left(\frac{k_{NN}^2}{2k_{N\Delta}^2}\right)\sigma(pp\to n\Delta^{++}), \quad (37)$$

where k_{NN} is the momentum in the NN center of mass, with the same energy as that available in the ΔN center of mass.

At very high T_Δ (i.e., above 2.5 GeV), other reaction channels such as $\Delta N \to \Delta\Delta$ open up, and the $\Delta N \to NN$ channel becomes relatively much less important. Hence at large T_Δ the above approximation for $\sigma_r^{\Delta N}$ is not accurate. At such energies we assume that the reaction dynamics for the Δ are the same as those of the proton at a kinetic energy enhanced by 300 MeV, i.e.,

$$\sigma_r^{\Delta N}(T_{\Delta N}) \approx \sigma_r^{NN}(T_{\Delta N} + 300\ \text{MeV}), \quad (38)$$

where $T_{\Delta N}$ is the total kinetic energy in the ΔN center-of-mass system. There is very little experimental information for the region $T_\Delta = 1.5$–2.5 GeV, so the Δ optical potentials at these energies are determined by interpolating between the values for W_Δ at $T_\Delta = 1.5$ and 2.5 GeV. The resultant W_Δ are listed in Table II.

TABLE I. Proton imaginary optical potential for various beam energies.

T_p (MeV)	W_p (MeV)
300	-28.3
400	-38.9
500	-50
800	-83.3
1000	-93.8
3000	-110.5

TABLE II. Δ imaginary optical potential for fixed mass $m_\Delta = 1220$ MeV.

T_Δ (MeV)	W_Δ (MeV)
< 60	-45
200	-34.6
400	-45
800	-52
1200	-55
1800	-64
2200	-95
3000	-107

C. Results and discussion

First we study the behavior of the double differential cross section as a function of the energy ω transferred to the nucleus. Assuming a fixed angle of 2° for the outgoing Δ in the (p,Δ^{++}) reaction, the cross sections are calculated using distorted waves and relativistic vertices, for incident beam energies of 1, 2, and 3 GeV. In Fig. 1 we plot $d^2\sigma/d\Omega\, d\omega$ as a function of ω. At 1 GeV we see a single peak in the cross section and two distinct peaks at 2 and 3 GeV beam energies. The peaks reflect the nuclear response convoluted with the available kinematics at a given energy. At the higher proton energies, the first peak is due to particle-hole $(N\,N^{-1})$ excitation whereas the second one is due to $(\Delta\,N^{-1})$ excitation in the nucleus. At 1 GeV we do not observe the second peak even though the energy transferred to the nucleus is sufficient to produce a Δ. This difference in the shape of the cross sections at 1 GeV and beyond can be understood by examining the overlap between the nuclear response and the allowed kinematic domain in the ω-q plane at a particular beam energy.

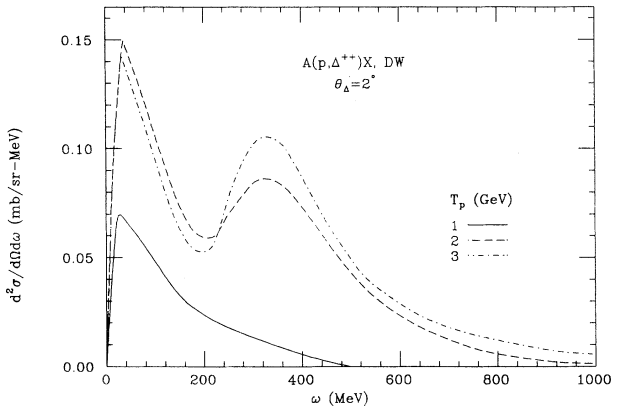

FIG. 1. Differential cross section, in mb/sr MeV, vs energy transfer to the nucleus ω, for the (p,Δ^{++}) reaction. Solid curve: proton beam energy of 1 GeV; dashed curve: proton energy of 2 GeV; dot-dashed curve: proton energy 3 GeV. Calculations are done for Δ emission angle of 2° relative to incident proton direction. Distorted waves are used for continuum particles, as described in the text. Unless otherwise specified calculations are done in the distorted-wave Fermi gas model, with $k_F = 210$ MeV. We assume short-range baryon-baryon repulsion of Migdal type with parameter $g' = 0.7$.

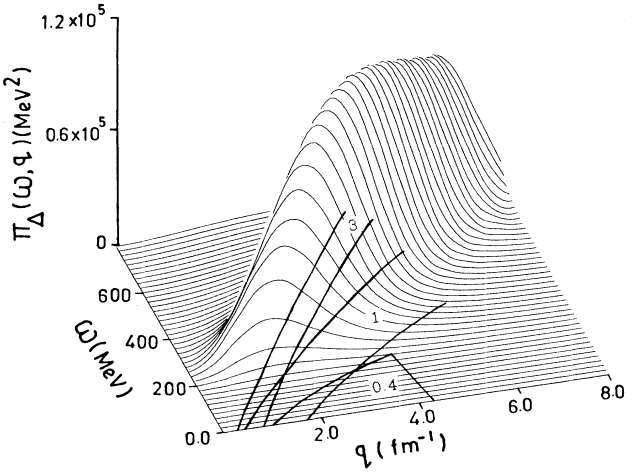

FIG. 2. Imaginary part of pion self-energy $\Pi_\Delta(\omega,q)$, in MeV^2, in nuclear matter as a function of energy transfer ω and momentum transfer q for isobar-hole (ΔN^{-1}) excitations. We assume short-range repulsion of Migdal type with parameter $g' = 0.7$. Pairs of lines denote the kinematic boundaries of (ω,q) for the (p,Δ^{++}) reaction at the beam energies listed in GeV, for Δ emission angle of 2°.

In Fig. 2 we plot the delta sector pion self-energy as a function of the energy transfer ω and momentum transfer $\mathbf{q}$. Since the calculation of $d^2\sigma/d\Omega\, d\omega$ involves an integral over μ, i.e., the effective mass of the delta, we have a range of q for each value of ω. Solid curves denote the kinematic boundaries for allowed range of ω-q for a Δ emitted at a 2° angle relative to the beam, for incident energies 0.4, 1, and 3 GeV. We observe that the ω-q domain at 3 GeV falls well within the area occupied by the delta response whereas the 1 GeV domain lies only at the edges and the 400 MeV domain lies totally outside the response. The mismatch between the Δ quasifree peak and the kinematically allowed region explains the energy dependence of the curves in Fig. 1.

In Fig. 3 we show the analogous curves for the nucleon

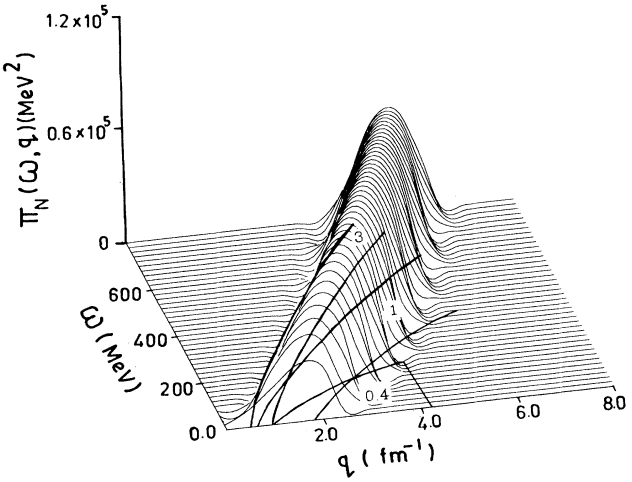

FIG. 3. Same as Fig. 2 for nucleon particle-hole excitations (NN^{-1}) assuming nucleon effective mass $m_N^* = 0.7m_N$.

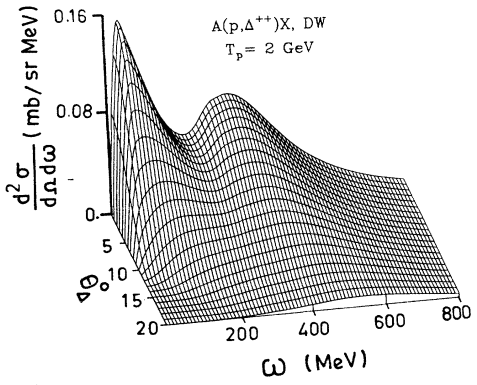

FIG. 4. Differential cross sections for the (p, Δ^{++}) reaction, in mb/sr MeV, as a function of energy transfer ω in MeV, and Δ emission angle in degrees. The proton incident energy is 2 GeV.

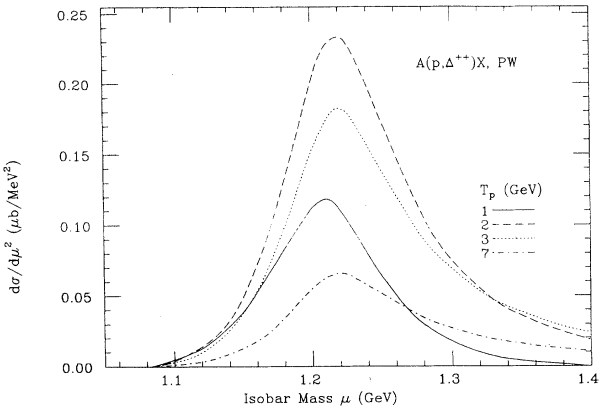

FIG. 5. Differential cross sections for (p, Δ^{++}) reaction vs the Δ mass, for proton beam energies 1–7 GeV. These calculations assume plane waves for the continuum particles. Solid curve: proton incident energy 1 GeV; dashed curve: proton energy 2 GeV; dotted curve: proton energy 3 GeV; dot-dashed curve: proton energy 7 GeV.

part of the self-energy. We see that both the 1 and 3 GeV regions overlap the response for small values of energy transfer ω. The 400 MeV kinematic domain also shows some small overlap with the response at low energy transfer. The maximum cross section at 1, 2, and 3 GeV beam energies is 70, 150, and 140 μb/sr MeV, respectively. The cross section at 400 MeV (not shown in Fig. 1) is very small with a peak value of only 3.6 μb/sr MeV.

In Fig. 4 we plot $d^2\sigma/d\Omega\, d\omega$ as a function of energy transfer and the angle of the outgoing Δ at incident beam energy $T_p = 2$ GeV. The cross sections fall with increasing angle of the delta and the two peaks seen as a function of ω at forward angles merge into one at large angles.

Plane-wave calculations of these cross sections as above give qualitatively the same results as our distorted-wave calculations. The difference due to distortion is essentially just a reduction in magnitude of the cross sections by a factor of 6 and 7 at $T_p = 1$ and 2 GeV, respectively, and by an order of magnitude at 3 GeV.

Finally, in Fig. 5 we show $d\sigma/d(\mu^2)$ as a function of μ, the mass of the Δ, for incident beam energies of 1, 2, 3, and 7 GeV. These cross sections are calculated with relativistic pion-nucleon coupling but without including the effects of distortions. The cross sections show a trend similar to that observed in the exclusive (p, Δ^{++}) reaction. The maximum in the cross section occurs at 2 GeV beam energy and cross sections fall on either side of this beam energy. Inclusion of distortions produces a reduction in the magnitude of the cross sections but no change in their shape. The reduction factors from distortions are approximately a factor of 6 at 1–2 GeV and a factor 8.6 at 3 GeV.

III. THE $(p, p'\pi^+)$ REACTION

A. Formalism

The Δ^{++} formed in the (p, Δ^{++}) reaction on the nucleus can be detected experimentally by measuring its decay products, the proton and pion, in coincidence. In this section we develop the theoretical framework and study the inclusive $(p, p'\pi^+)$ reaction with a Δ^{++} formed in the intermediate state. The formalism for this reaction is developed along lines similar to the inclusive (p, Δ^{++}) reaction.

The cross section for the inclusive $(p, p'\pi^+)$ reaction, shown schematically in Fig. 6, is written in terms of the one-pion-exchange interaction which converts the incident proton to a Δ^{++}, the delta propagator, its decay vertex, and the response of the nucleus.

The transition amplitude T_{n0} was discussed in Sec. II; the factorized form of this amplitude with the nonrelativistic reduction of the $\pi N\Delta$ vertices has the form

$$T_{n0} = \frac{f^*}{m_\pi} V(\mathbf{q},\omega) \langle p'|\mathbf{S}\cdot\mathbf{k}_\pi \mathbf{T}_-|\Delta^{++}\rangle \frac{1}{D_\Delta} \langle \Delta^{++}|\mathbf{S}^\dagger\cdot\hat{\mathbf{q}}\mathbf{T}_+^\dagger|p\rangle F_{n0}(-q). \tag{39}$$

D_Δ is the delta propagator which in the nonrelativistic form is written as $(M^* - m_\Delta - i\Gamma/2)$, where M^* is the resonance mass equal to 1232 MeV and m_Δ is the varying mass of the Δ. The free width of the resonance is $\Gamma = 116$ MeV. The quantities $V(\omega, \mathbf{q})$ and $F_{n0}(-q)$ are evaluated as described in Sec. II. Taking $\mathbf{k}_p$ to be along the z direction and assuming coplanar geometry for the final state, we obtain

$$\sum_n \delta(\omega-\omega_n) \sum_{\sigma_p \sigma_{p'}} |T_{n0}|^2 = \frac{2}{9}\frac{f^{*2}}{m_\pi^2} |V(\mathbf{q},\omega)|^2 \frac{1}{D_\Delta^2} \left\{k_\pi^2(1+3\cos^2\theta_q)\right\} S(\mathbf{q},\omega). \tag{40}$$

Here θ_q is the angle between the vectors $\mathbf{q}$ and $\mathbf{k}_\pi$. Using the relativistic interaction at the $\pi N\Delta$ vertices we get the following expression for the transition amplitudes:

$$\sum_n \delta(\omega-\omega_n)\sum_{\sigma_p\sigma_{p'}}|T_{n0}|^2=\frac{2}{9}\frac{f^{*2}}{m_\pi^2}|V(\mathbf{q},\omega)|^2\frac{1}{D_\Delta^2}R(\mathbf{q},\omega)S(\mathbf{q},\omega), \tag{41}$$

where $R(\mathbf{q},\omega)$ is defined by

$$R(\mathbf{q},\omega)=\frac{3}{4}\frac{m_\pi^2}{m_p^2 m_\Delta}\frac{1}{\mathbf{q}^2}\left[-t+\frac{(t-m_p^2+m_\Delta^2)^2}{4m_\Delta^2}\right]\times\left\{m_p\left[t-2m_p^2-2m_\Delta^2+m_\pi^2\right]+m_\Delta\left[t+m_\pi^2-4m_p^2-2(\mathbf{q}\cdot\mathbf{k}_\pi-\omega E_\pi)\right]\right\}. \tag{42}$$

The relativistic form of the Δ propagator is written as

$$D_\Delta^2=\frac{(m_\Delta^2-M^{*2})^2+\Gamma^2M^{*2}}{4M^{*2}}. \tag{43}$$

B. Cross sections

The differential cross section for the inclusive $(p,p'\pi^+)$ reaction at a given outgoing proton energy is given as

$$\frac{d^4\sigma}{dE_\pi d\Omega_\pi dE_{p'}d\Omega_{p'}}=\frac{m_p^2}{2(2\pi)^5}\frac{k_{p'}k_\pi}{k_p}\sum_n\delta(\omega-\omega_n)\frac{1}{2}\sum_{\sigma_p\sigma_{p'}}|T_{n0}|^2, \tag{44}$$

where $\omega=E_p-E_{p'}-E_\pi$ is the energy transferred to the nucleus. $E_{p'}$ and E_π are the energies and $\Omega_{p'}$ and Ω_π are the solid angles for the outgoing proton and pion with respect to the incident proton direction. The energy spectrum for the proton in the final state is calculated by integrating Eq. (44) over the allowed range of energy of the pion and the pion angle.

An integral over the pion energies implies an integral over a range of energy transfer ω. The limit on this integral, i.e., $\omega_{\max}$, at a particular beam energy is taken as the value of ω where the (p,Δ^{++}) cross section becomes negligible. This ensures that the calculation of the $(p,p'\pi^+)$ cross section lies in the region dominated by Δ production in the intermediate state.

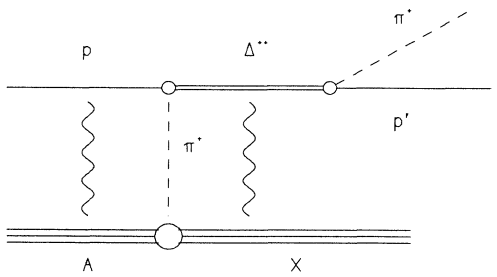

FIG. 6. Schematic diagram for the $A(p,p'\pi^+)X$ reaction. The incident proton is excited to Δ, which decays to nucleon plus pion. Wavy lines denote hadron-nucleus distortions.

C. Results and discussion

First we calculate the proton spectrum for the $(p,p'\pi^+)$ reaction. In Fig. 7 $d^2\sigma/d\Omega\, p'dEp'$, as a function of outgoing proton kinetic energy, $T_{p'}$, is shown for beam energies of 1, 2, and 3 GeV. The calculations are done using the relativistic distorted-wave formalism. The angle of the outgoing proton is fixed at 5°. These results show a single peak in the cross section at 1 GeV, developing into two distinct peaks at 2 and 3 GeV. However, these two peaks do not belong separately to the nucleon and Δ excitations in the nucleus. Both of them, in fact, receive contributions from both the nucleon and Δ sectors of the nuclear response. This happens because for each energy $T_{p'}$ of the outgoing proton there is a range of allowed values of the pion energy, and there is a corresponding range of energy transfer ω to the nucleus. This gives rise to contributions to the cross section from the nuclear response at low ω (nucleon sector) as well as higher ω (delta sector) for each value of $T_{p'}$.

The nucleon and delta response in the $(p,p'\pi^+)$ experiment can be separated, however, if the measurements are done in a kinematically complete geometry. In Fig. 8 we show results with fixed angles for the π^+ and proton and a fixed value of the outgoing proton energy. The

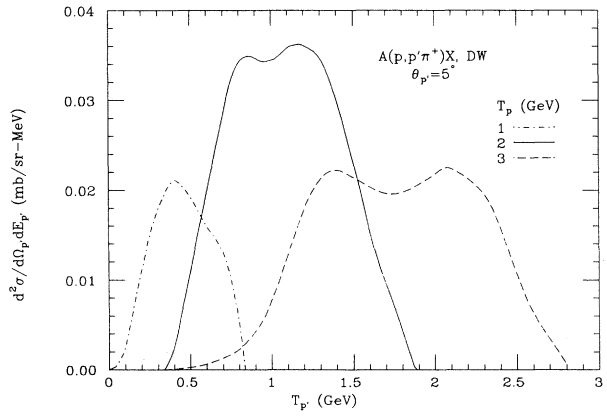

FIG. 7. Energy spectrum of outgoing proton in the $(p,p'\pi^+)$ reaction, in mb/sr MeV. The outgoing proton angle is 5° relative to beam direction; calculations have been carried out for incident proton energies 1 GeV (dot-dashed curve), 2 GeV (solid curve), and 3 GeV (dashed curve); the cross sections have been integrated over the energy and angle of the outgoing pion.

cross section $d^4\sigma/d\Omega_\pi d\Omega_{p'} dE_{p'} dE_\pi$ is shown as a function of pion energy (equivalently energy transfer ω), for incident energy $T_p = 1$, 2, and 3 GeV. The angle between the incident and outgoing protons is kept fixed at $-10°$ and that of the pion at $+10°$ relative to the beam, i.e., in the reaction plane the proton and pion come out on opposite sides with respect to the incident beam direction. The above choice of angles is made because the cross sections peak for forward pion and proton angles. The energies of the outgoing protons are fixed at 290, 870, and 1700 MeV for incident beam energies of 1, 2, and 3 GeV, respectively. These energies of the proton correspond to the positions of the peak in the cross sections, $\left(\int \left[d^4\sigma/d\omega\, d\Omega_\pi d\Omega_{p'} dE_{p'}\right] d\omega\right)$ as a function of $T_{p'}$.

In Fig. 8, as in Fig. 1, two distinct peaks are seen in the cross section for incident energy 2 and 3 GeV, and only a single peak at 1 GeV and below. The first peak in all cases corresponds to quasielastic nucleon excitation in the nucleus, and the second peak at 2 and 3 GeV is due to Δ excitation in the nuclear response. The enhancement in the cross section for the second peak arises due to the delta propagator, D_Δ, in Eq. (41). In the kinematics considered in this paper, each value of the energy transfer ω to the nucleus corresponds to a certain value of the Δ mass. The region of ω which produces the second peak at 2 and 3 GeV corresponds to the delta mass in the vicinity of its resonant mass M^*. The maximum cross sections at 1, 2, and 3 GeV are 0.1, 0.23, and 0.34 μb/sr^2 MeV^2. The calculations at 400 MeV beam energy (not shown) exhibit a single peak with small cross section 0.012 μb/sr^{2}MeV^2.

To show in more detail how the second peak grows with increasing beam energy, in Fig. 9 we show the excitation spectrum of the nucleus for 1.0, 1.2, and 1.5 GeV beam energies. At 1 GeV there is little indication of the Δ-response peak, while at 1.2 GeV it develops into a clear

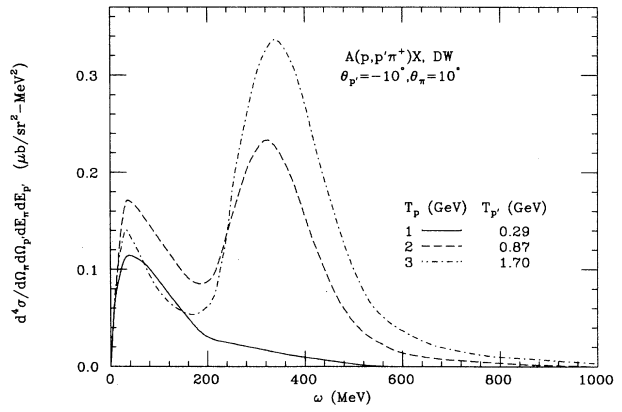

FIG. 8. Differential cross sections for the $(p, p'\pi^+)$ reaction, in μb/sr^2 MeV^2, as a function of energy transfer ω to the nucleus. The proton and pion are detected at fixed angles of 10° on either side of the beam direction. The energies of the outgoing protons are chosen to correspond to maxima in the outgoing proton energy spectrum. Solid curve: incident proton energy 1 GeV ($T_{p'} = 290$ MeV); dashed curve: proton energy 2 GeV ($T_{p'} = 870$ MeV); dot-dashed curve: proton energy 3 GeV ($T_{p'} = 1.70$ GeV).

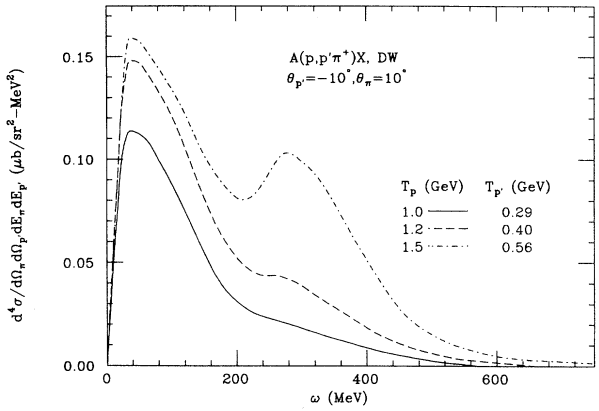

FIG. 9. Same as Fig. 8. Solid curve: proton incident beam energy 1.0 GeV ($T_{p'} = 290$ MeV); dashed curve: proton incident energy 1.2 GeV ($T_{p'} = 400$ MeV); dot-dashed curve: proton incident energy 1.5 GeV ($T_{p'} = 560$ MeV).

shoulder and then by 1.5 GeV into a distinct bump. A peak will be observed in this reaction when the energy-momentum transfer matches the location of the Δ peak in the nuclear response Π_Δ, shown in Fig. 2. For 1 GeV beam energy the allowed kinematic region does not include the Δ peak, but with increasing energy the energy-momentum transfer includes the Δ response peak and a bump appears in the experimental cross section.

This situation is similar to the inclusive 0° $(^3\mathrm{He}, t)$ experiments conducted earlier on ^{12}C for beam energies 1.5–2.3 GeV [6]. At 1.5 GeV ^{3}He incident energy a clear Δ peak was not seen in the $(^3\mathrm{He}, t)$ reaction even though the energy was sufficient to excite a Δ. At 1.5 GeV incident energy the energy momentum transfer in this reaction does not include the Δ peak; the overlap with the Δ peak in the nuclear response improved with increasing beam energy.

Finally, we may recollect that all results shown so far are calculated using a cutoff parameter $\Lambda = 1.2$ GeV/c for both the πNN and $\pi N\Delta$ vertices. In Figs. 10 and

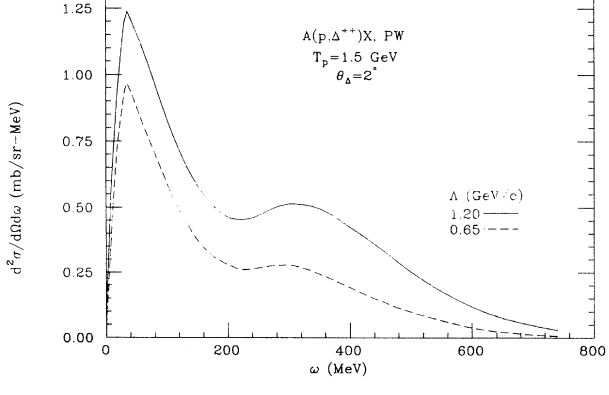

FIG. 10. Sensitivity of the differential cross section, in mb/sr MeV, in the (p, Δ^{++}) reaction to the cutoff momentum Λ at the $N\pi$ vertex. Solid curve: $\Lambda = 1.2$ GeV; dashed curve: $\Lambda = 0.65$ GeV. Proton incident energy $T_p = 1.5$ GeV and scattering angle $\theta_\Delta = 2°$.

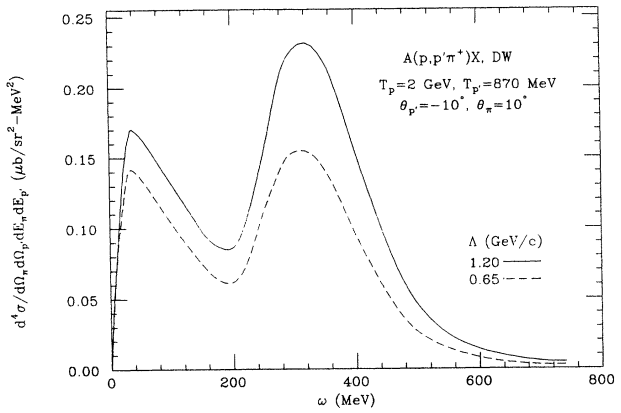

FIG. 11. Sensitivity of the differential cross section, in μb/sr^2 MeV^2, in the $(p,p'\pi^+)$ reaction to the cutoff momentum Λ at the $N\pi$ vertex. Solid curve: $\Lambda = 1.2$ GeV; dashed curve: $\Lambda = 0.65$ GeV. Proton incident and outgoing energies $T_p = 2$ GeV and $T_{p'} = 0.87$ GeV, respectively; outgoing proton and pion angles $\theta_{p'} = -10°$ and $\theta_\pi = 10°$.

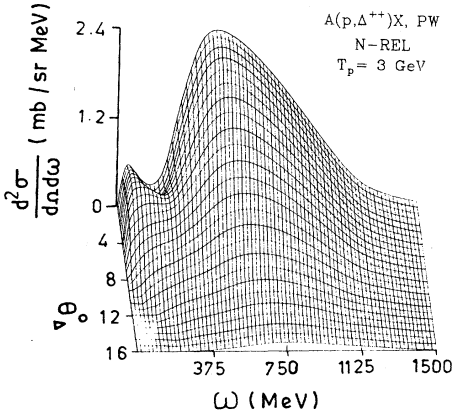

FIG. 12. Differential cross section, in mb/sr MeV, for the (p,Δ^{++}) reaction at proton beam energy 3 GeV, using nonrelativistic pion-nucleon coupling at all vertices, and plane waves for continuum particles.

11 we show the sensitivity of the excitation spectra for the $(p,p'\pi^+)$ and (p,Δ^{++}) reactions to the value of Λ. The cross sections are given for $\Lambda = 1.2$ and 0.65 GeV/c. It is observed that the reduction in the value of Λ leads to an overall reduction in the magnitude of the cross sections. This is understandable because the smaller Λ gives a form factor which is deficient in high momentum components, and in the (p,Δ^{++}) reaction these are the momenta which are relevant.

IV. RELATIVISTIC VS NONRELATIVISTIC COUPLING VERTICES

In Δ production it is common to use the static nonrelativistic reduction of the pion-nucleon interaction vertex, because of its relative simplicity. At low energies this may give reliable results; for higher energies, this approximation can be quite inaccurate. In this section we review those kinematic regions where the static nonrelativistic reduction can give unreliable results and we calculate the extent of the differences between relativistic and nonrelativistic calculations.

In Figs. 12 and 13 we show $d^2\sigma/d\omega\, d\Omega$ for the (p,Δ^{++}) reaction at 3 GeV beam energy, as a function of the energy transfer ω and angle of the Δ. The two figures compare the nonrelativistic and relativistic pion-nucleon couplings using plane waves for the incident and outgoing particles. The two figures are very different. In the relativistic calculations the peak cross sections in the region of the quasielastic nucleon response are larger than those for the Δ response; this situation is reversed in the static nonrelativistic calculations. In addition, the magnitudes of the calculations are quite different. Similar results are found at 1 GeV beam energy. For a proton beam energy of 400 MeV, however, the relativistic and nonrelativistic couplings produce similar results.

To understand the large difference observed between our relativistic and static nonrelativistic results we examine the effect of the nonrelativistic reduction which arises in three places:

(i) the $p \to \Delta^{++}$ transition,

(ii) the pion self-energy in the nuclear medium, and

(iii) the $\Delta^{++} \to p\pi^+$ decay.

We first examine the $p \to \Delta^{++}$ transition vertex. As shown in the Appendix, relativistic coupling for this vertex gives

$$\overline{|\Gamma_{\Delta N\pi}|^2} = \left(\frac{f^*}{m_\pi}\right)^2 \left[\frac{t-(m_p+m_\Delta)^2}{6m_p m_\Delta}\right]\left[t - \frac{(t-m_p^2+m_\Delta^2)^2}{4m_\Delta^2}\right] \tag{45}$$

while for the static nonrelativistic coupling

$$\overline{|\Gamma_{\Delta N\pi}|^2_{\rm NR}} = \left(\frac{f^*}{m_\pi}\right)^2 \frac{2\mathbf{q}^2}{3}. \tag{46}$$

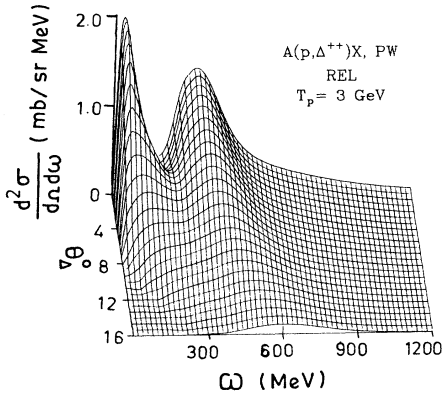

FIG. 13. Same as Fig. 12 for relativistic pion-nucleon coupling.

We show in the Appendix that the relativistic and nonrelativistic results agree when $E/m \sim 1$, and when $k/m \sim 0$ for both nucleon and isobar. While these conditions may be met near the delta threshold, they are likely to be strongly violated for proton beam energies of 1 GeV and higher. For real pions the final factor in Eq. (45) is the square of the relative pion-nucleon momentum in the isobar rest frame. Inclusion of nucleon recoil in Eq. (46) would restore some of the agreement between relativistic and nonrelativistic descriptions of this process, but there may still be substantial disagreement between relativistic and nonrelativistic results for proton beam energies of 1 GeV and higher.

As an illustration, consider the region of very small energy transfer ω to the nucleus. For proton incident energies of 1 GeV, 3 GeV, and 7 GeV the momentum transfer $\mathbf{q}$ is 217, 100, and 56 MeV/c, respectively, for a ^{16}O target. For these kinematics Eq. (45) can be approximated as

$$\overline{|\Gamma_{\Delta N\pi}|^2} \approx \left(\frac{f^*}{m_\pi}\right)^2 \frac{2}{3}\left(\mathbf{q}^2 + [258\ \text{MeV}]^2\right). \qquad (47)$$

Compared to the static nonrelativistic expression, Eq. (46), which is proportional to $\mathbf{q}^2$, the relativistic expression in this region is significantly larger than the static nonrelativistic result. For momentum transfers appropriate for the (p, Δ^{++}) reaction on ^{16}O, the ratio of relativistic to nonrelativistic predictions would be about 2.4, 7.5, and 22 for proton beam energies of 1, 3, and 7 GeV, respectively. The static nonrelativistic approximations would then significantly underestimate these cross sections, and would also predict a dependence on momentum transfer not seen in the relativistic calculations.

To exhibit the difference due to relativistic and nonrelativistic expressions for the pion self-energy, in Fig. 14 we show $d\sigma/d\omega\, d\Omega$ for the (p, Δ^{++}) reaction at $\theta_\Delta = 2°$ and 3 GeV beam energy. The two curves correspond to the relativistic and nonrelativistic versions of the pion self-energy $\Pi(\omega, \mathbf{q})$. In both cases we use the nonrelativistic $p \rightarrow \Delta^{++}$ transition vertex. We see that the

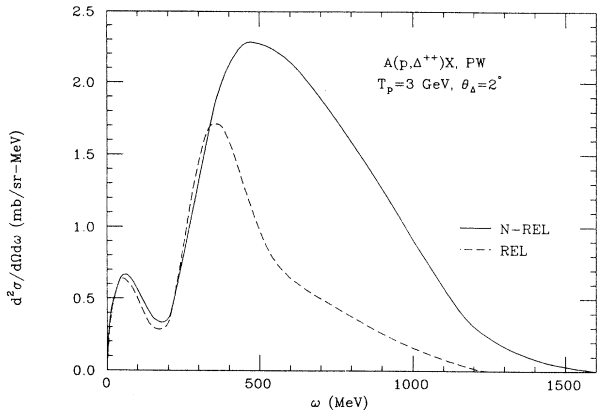

FIG. 14. Sensitivity of the nuclear excitation spectrum in the (p, Δ^{++}) reaction to the treatment of pion self-energy in the nucleus. Both curves use static nonrelativistic $\Delta N\pi$ coupling. Solid curve: nonrelativistic evaluation of pion self-energy; dashed curve: relativistic form of pion self-energy. Incident proton energy $T_p = 3$ GeV and Δ scattering angle $\theta_\Delta = 2°$.

nonrelativistic approximation to the self-energy is good at small ω when it receives contributions from nucleon particle-hole (NN^{-1}) excitations only. The second peak in $d^2\sigma/d\Omega\, d\omega$ at higher energy transfer, which is mainly due to Δ-hole (ΔN^{-1}) excitations, is significantly overestimated in the nonrelativistic approximation to the pion self-energy. Thus combining the above effects of the nonrelativistic approximations to the $p \rightarrow \Delta^{++}$ vertex and the pion self-energy, we can straightforwardly understand the significant differences observed between the relativistic and nonrelativistic calculations shown in Figs. 12 and 13.

For the $(p, p'\pi^+)$ reaction we have the additional decay vertex of the isobar into proton and pion. In the static nonrelativistic reduction this vertex gives a contribution of $(4/3)\mathbf{k}_\pi^2$, while in the relativistic case the same vertex gives

$$\overline{|\Gamma_{\Delta N\pi}|^2} = \frac{1}{3m_p m_\Delta}\left[m_\pi^2 - \frac{(m_\pi^2 + m_\Delta^2 - m_p^2)^2}{4m_\Delta^2}\right]\left[m_\pi^2 - (m_p + m_\Delta)^2\right] \approx \frac{4}{3}m_\pi^2. \qquad (48)$$

Thus whenever k_π is very large ($\gg m_\pi$) the nonrelativistic form of the vertex significantly overestimates the cross sections. Calculation of the proton energy spectra $d^2\sigma/d\Omega_{p'}dE_{p'}$ at each $E_{p'}$ involves an integral over the pion energy E_π. The values of E_π and their allowed range become larger as the beam energy increases.

V. SUMMARY

We have outlined the formalism for the inclusive (p, Δ^{++}) and $(p, p'\pi^+)$ reactions and calculated the cross sections for them. These reactions provide an opportunity to study the response of the nucleus over a wide range of energy and momentum transfer. The shapes of the calculated cross sections reflect the behavior of the nuclear response in various situations.

In the (p, Δ^{++}) reaction, we observe the excitation of the Δ isobar in the nucleus for beam energies of 2 and 3 GeV. At 1 GeV no such Δ excitation is observed despite the fact that the excitation energy is sufficient to produce a Δ. We showed that this occurred because of the mismatch between the energy-momentum transferred to the nucleus in this reaction, and the position of the nuclear response in the $(\mathbf{q}, \omega)$ plane. However, the quasielastic nucleon peak is observed at all beam energies. As a function of the Δ missing mass, cross sections

for the inclusive (p,Δ^{++}) reaction reach a maximum value at 2 GeV beam energy.

As the experimental observation of the Δ^{++} in the inclusive (p,Δ^{++}) reaction requires a coincidence measurement of its decay products (proton and pion), we calculated cross sections for the $(p,p'\pi^+)$ reaction at different kinematics which should be useful for planning future inclusive experiments.

The inclusive proton energy spectrum in the $(p,p'\pi^+)$ reaction, unlike the inclusive spectra in (p,p') and (p,Δ^{++}) reactions, do not show separate peaks due to quasielastic nucleon and quasielastic Δ excitation in the nucleus. This occurs because a particular energy of the final state proton in the $(p,p'\pi^+)$ reaction can correspond to various energies of the intermediate Δ and hence various values of energy transfer. Therefore the energy spectrum of the proton has contributions from the nucleon and delta-hole excitations in the nucleus for all values of $E_{p'}$. However, in $(p,p'\pi^+)$ reactions the two branches of the nuclear response can be separated, if the proton and pion are detected at fixed angles and measurements are made at a fixed value of the proton energy. The nucleon and Δ^{++} sectors in this case are well separated.

The results of our models underscore the importance of using relativistic approximations at all possible stages in calculating cross sections. We showed that nonrelativistic forms of transition vertices not only gave incorrect estimates of the magnitudes but even failed to predict the correct shape of the cross sections.

Finally, we showed that inclusion of distortions in these reactions reduce the magnitude of the cross sections but do not change the shape of our calculated results.

ACKNOWLEDGMENTS

One of the authors (B.K.J.) wishes to thank the Indiana University Nuclear Theory Center for its hospitality and support during his visits to the Center. One of the authors (N.G.K.) gratefully acknowledges the award of a research fellowship from the Department of Atomic Energy of the Government of India. One of the authors (J.T.L.) was supported in part by the U.S. National Science Foundation under Contract No. NSF-PHY91-08036. The authors wish to thank V. F. Dmitriev for useful discussions, and thank J. Cartwright for assistance with the figures for this paper.

APPENDIX: RELATIVISTIC AND NONRELATIVISTIC π AND Δ VERTICES

The coupling of pions to nucleons and Δ is defined through the Lagrangians which (assuming pseudovector $NN\pi$ coupling) have the form

$$\mathcal{L}_{NN\pi} = \frac{f}{m_\pi}\overline{\Psi}_N\gamma^\nu\gamma^5\boldsymbol{\tau}\Psi_N\cdot\partial_\nu\boldsymbol{\phi}, \tag{A1}$$

$$\mathcal{L}_{\Delta N\pi} = \frac{f^*}{m_\pi}\overline{\Psi}^\nu_\Delta\mathbf{T}\Psi_N\cdot\partial_\nu\boldsymbol{\phi}. \tag{A2}$$

Here $\boldsymbol{\phi}$ is the pion isovector field, Ψ_N is the nucleon spinor, Ψ^ν_Δ is the Rarita-Schwinger field for the Δ isobar, and $\mathbf{T}$ is the isospin transition operator for the $1/2\rightarrow 3/2$ transition. Frequently nucleon and Δ transitions are described using the nonrelativistic reductions of these vertices,

$$H_{NN\pi} = i\frac{f}{m_\pi}\boldsymbol{\sigma}\cdot\mathbf{q}\boldsymbol{\tau}\cdot\boldsymbol{\phi}, \tag{A3}$$

$$H_{\Delta N\pi} = i\frac{f^*}{m_\pi}\mathbf{S}\cdot\mathbf{q}\mathbf{T}\cdot\boldsymbol{\phi}. \tag{A4}$$

In Eq. (A4), $\mathbf{S}$ is the spin transition operator analogous to $\mathbf{T}$.

The nonrelativistic reductions of these couplings should be generally valid whenever the nucleon or isobar momenta are small relative to their rest masses, and when energy transfers at the vertices are also small. For our calculations neither of these conditions holds; we are looking at proton incident kinetic energies of 1 GeV or greater, and for production of Δ near the resonant mass the energy transfer at the $\Delta N\pi$ vertex is generally large. In order to quantify the accuracy of the nonrelativistic approximations, we derive kinematic equations which relate relativistic and nonrelativistic amplitudes as they contribute to various calculated cross sections.

First we calculate the relativistic $NN\pi$ amplitude. If we evaluate the term of Eq. (A1) to a cross section for unpolarized nucleons, we square the amplitude and average over spins which gives

$$\begin{aligned}\overline{|\Gamma_{NN\pi}(t)|}^2 &\equiv \frac{1}{2}\sum_{\text{spins}}|\langle N\pi\rightarrow N\rangle|^2\\ &= \frac{2f^2}{m_\pi^2}\left(m_N^2 - k_N\cdot k'_N\right)\\ &= \frac{f^2}{m_\pi^2}\left[\omega^2-\mathbf{q}^2\right].\end{aligned} \tag{A5}$$

As is well known, the relativistic $NN\pi$ vertex depends on the energy ω and momentum $\mathbf{q}$ carried by the pion. When the pion energy is small relative to its three-momentum this vertex just reduces to the nonrelativistic form,

$$\overline{|\Gamma_{NN\pi}(t)|}^2 = -\frac{f^2}{m_\pi^2}\mathbf{q}^2$$

(where we have neglected nucleon recoil momentum terms in the nonrelativistic reduction).

For the $\Delta N\pi$ vertex, squaring the amplitude from Eq. (A2) and averaging over spins gives

$$\begin{aligned}\overline{|\Gamma_{\Delta N\pi}(t)|}^2 &\equiv \frac{1}{2}\sum_{\text{spins}}|\langle p\pi^+\rightarrow\Delta^{++}\rangle|^2\\ &= -\left(\frac{f^*}{m_\pi}\right)^2 q_\mu q_\nu\,\mathrm{Tr}\left[\frac{\not{k}+m_p}{2m_p}\left(\frac{\not{k}_\Delta+m_\Delta}{2m_\Delta}\right)D^{\mu\nu}(k_\Delta)\right],\end{aligned} \tag{A6}$$

where

$$D^{\mu\nu}(k_\Delta) \equiv g^{\mu\nu} - \tfrac{1}{3}\gamma^\mu\gamma^\nu - 2k_\Delta^\mu k_\Delta^\nu/3m_\Delta^2 + (k_\Delta^\mu\gamma^\nu - k_\Delta^\nu\gamma^\mu)/3m_\Delta.$$

Evaluation of Eq. (A6) gives

$$\begin{aligned}\overline{|\Gamma_{\Delta N\pi}(t)|}^2 &= -\frac{1}{3}\left(\frac{f^*}{m_\pi}\right)^2\left(1+\frac{k\cdot k_\Delta}{m_p m_\Delta}\right)\left[q^2-\left(\frac{k_\Delta\cdot q}{m_\Delta}\right)^2\right] \\ &= -\frac{1}{3}\left(\frac{f^*}{m_\pi}\right)^2\left[1+\frac{m_\Delta^2+m_p^2-t}{2m_p m_\Delta}\right]\left[t-\left(\frac{m_\Delta^2-m_p^2+t}{2m_\Delta}\right)^2\right]. \end{aligned} \tag{A7}$$

Expanding the four vectors in Eq. (A7) gives

$$\begin{aligned}\overline{|\Gamma_{\Delta N\pi}(t)|}^2 = &-\frac{1}{3}\left(\frac{f^*}{m_\pi}\right)^2\left[1+\frac{E_N E_\Delta - \mathbf{k}\cdot\mathbf{k}_\Delta}{m_p m_\Delta}\right] \\ &\times\left(\omega^2-\mathbf{q}^2-\left[\frac{\omega E_\Delta - \mathbf{k}_\Delta\cdot\mathbf{q}}{m_\Delta}\right]^2\right).\end{aligned} \tag{A8}$$

The static nonrelativistic reduction of the $\Delta N\pi$ vertex can be shown to give a contribution

$$\overline{|\Gamma_{\Delta N\pi}(t)|}^2_{\rm NR} = \left(\frac{f^*}{m_\pi}\right)^2\frac{2\mathbf{q}^2}{3}.$$

Equation (A8) reduces to the NR values whenever $E/m \sim 1$ and $k/m \sim 0$ for both nucleon and isobar; for example, production of a real isobar near threshold would satisfy this requirement. For real pions the last term in Eq. (A7) is the square of the relative pion-nucleon momentum in the isobar rest frame; in this case replacing the pion momentum $\mathbf{q}$ by the relative π-N momentum will give a reasonable approximation to the relativistic result.

[1] See, e.g., Proceedings of the First Yukawa International Seminar, Kyoto, 1987, edited by H. Ohtsubo and T. Suzuki [Prog. Theor. Phys. (Suppl.) **91** (1987)].

[2] T.E.O. Ericson and W. Weise, *Pions and Nuclei* (Clarendon, Oxford, 1988).

[3] E. Oset, H. Toki, and W. Weise, Phys. Rep. **83**, 281 (1982); A.B. Migdal, E.E. Sapirstein, M.A. Troitsky, and D.N. Voskresensky, *ibid.* **192**, 179 (1990).

[4] B.E. Bonner, J.E. Simmons, C.R. Newsom, P.J. Riley, G. Glass, J.C. Hiebert, Mahavir Jain, and L.C. Northcliffe, Phys. Rev. C **18**, 1418 (1978).

[5] C. Ellegaard *et al.*, Phys. Rev. Lett. **50**, 1745 (1983); I. Bergqvist *et al.*, Nucl. Phys. **A469**, 648 (1987); C. Ellegaard *et al.*, Phys. Lett. **154B**, 110 (1985).

[6] D. Contardo *et al.* Phys. Lett. **168B**, 331 (1986).

[7] D. Bachelier *et al.*, Phys. Lett. B **172**, 23 (1986).

[8] T. Udagawa, S-W. Heng, and F. Osterfeld, Phys. Lett. B **245**, 1 (1990); J. Delorme, in *Proceedings of the Seventh International Conference on Polarization Phenomena in Nuclear Physics*, edited by A. Boudard and Y. Terrien (Les Editions de Physique, Paris, 1990); V.F. Dmitriev, Budker Institute of Nuclear Physics, Report 92-20, 1992.

[9] J. Chiba *et al.*, Phys. Rev. Lett. **67**, 1982 (1991); T. Hennino, Nucl. Phys. **A527**, 399c (1991); T. Hennino *et al.*, Phys. Lett. B **283**, 42 (1992).

[10] T. Hennino *et al.*, Phys. Rev. Lett. **48**, 997 (1982); C. Gaarde, *Proceedings of the International Conference on Nuclear Physics, Harrogate, 1986*, edited by J. L. Durrell, J. M. Irving, and G. C. Morrison (Hilger, London, 1986).

[11] V.G. Ableev *et al.*, Pis'ma Zh. Eksp. Teor. Fiz. **40**, 35 (1984) [JETP Lett. **40**, 763 (1984)].

[12] V.F. Dmitriev, O. Sushkov, and C. Gaarde, Nucl. Phys. **A459**, 503 (1986).

[13] H. Esbensen and T.H.S. Lee, Phys. Rev. C **32**, 1966 (1985); E. Oset, E. Shino, and H. Toki, Phys. Lett. B **224** 249 (1989); V.F. Dmitriev and T. Suzuki, Nucl. Phys. **A438**, 697 (1985).

[14] B.K. Jain, Phys. Rev. Lett. **50**, 815 (1983); Phys. Rev. C **29**, 1396 (1984); **32**, 1253 (1985); B.K. Jain and A.B. Santra, Nucl. Phys. **A500**, 681 (1989).

[15] B.K. Jain, N.G. Kelkar, and J.T. Londergan, Phys. Rev. C **43**, 271 (1991).

[16] N.G. Kelkar and B.K. Jain, Phys. Rev. C **46**, 845 (1992).

[17] R.D. Smith, in *Spin Observables of Nuclear Probes*, edited by C.J. Horowitz, C.D. Goodman, and G.E. Walker (Plenum, New York, 1988), p. 15.

[18] A.B. Wicklund, M.W. Arenton, D.S. Ayres, R. Diebold, S.L. Kramer, E.N. May, L.J. Nodulman, and J.R. Sauer, Phys. Rev. D **34**, 19 (1986); A.B. Wicklund *et al.*, *ibid.* **35**, 2670 (1987).

[19] C. Ellegaard *et al.*, Phys. Lett. B **231**, 365 (1989).

[20] B.K. Jain and A.B. Santra, Phys. Rev. C **46**, 1183 (1992).

[21] T. Sams and V.F. Dmitriev, Phys. Rev. C **45**, R2555 (1992).

[22] T.E.O. Ericson and M. Rosa-Clot, Nucl. Phys. **A405**, 497 (1983); Annu. Rev. Nucl. Part. Sci. **35**, 271 (1985).

[23] C.A. Dominguez and B.J. VerWest, Phys. Lett. B **89**, 333 (1980); K. Holinde, Phys. Rep. **68**, 121 (1981).

[24] B.K. Jain and A.B. Santra, Nucl. Phys. **A519**, 697 (1990).

[25] S. Kumano, Phys. Rev. D **43**, 59 (1991); A.W. Thomas, Phys. Lett. **126B**, 97 (1983); M. Ericson and A.W.

Thomas, *ibid.* **148B**, 191 (1984); L.L. Frankfurt, L. Mankiewicz, and M.I. Strikman, Z. Phys. A **334**, 343 (1989); S. Kumano, Phys. Rev. D **41**, 195 (1990).

[26] A. Fetter and J.D. Walecka, *Quantum Theory of Many Particle Systems* (McGraw-Hill, New York, 1971).

[27] B.K. Jain, J.T. Londergan, and G.E. Walker, Phys. Rev. C **37**, 1564 (1988).

[28] D.V. Bugg, D.C. Salter, G.H. Stafford, R.F. George, K.F. Riley, and R.J. Tapper, Phys. Rev. **146**, 980 (1966); S. Barshay, C.B. Dover, and J.P. Vary, Phys. Rev. C **11**, 360 (1975); K. Chen, G. Friedlander, J.R. Grover, J.M. Miller, and Y. Shimamoto, Phys. Rev. **166**, 949 (1968).

[29] F. Shimizu, Y. Kubota, H. Koiso, F. Sai, S. Sakamoto, and S.S. Yamamoto, Nucl. Phys. **A386**, 571 (1982); F. Shimizu, H. Koiso, Y. Kubota, F. Sai, S. Sakamoto, and S.S. Yamamoto, *ibid.* **A389**, 445 (1982).

[30] M. Hirata, F. Lenz, and K. Yazaki, Ann. Phys. (N.Y.) **108**, 116 (1977); Y. Horikawa, M. Thies, and F. Lenz, Nucl. Phys. **A435**, 386 (1980).